Full Counting Statistics in a Propagating Quantum Front and Random Matrix Spectra

Viktor Eisler
Vienna Center for Quantum Science and Technology, Faculty of Physics, University of Vienna, Boltzmanngasse 5, A-1090 Wien, Austria

Zoltán Rácz
Institute for Theoretical Physics-HAS, Eötvös University, Pázmány sétány 1/a, 1117 Budapest, Hungary
(Received 20 November 2012; published 5 February 2013)

One-dimensional free fermions are studied with emphasis on propagating fronts emerging from a step initial condition. The probability distribution of the number of particles at the edge of the front is determined exactly. It is found that the full counting statistics coincide with the eigenvalue statistics of the edge spectrum of matrices from the Gaussian unitary ensemble. The correspondence established between the random matrix eigenvalues and the particle positions yields the order statistics of the rightmost particles in the front and, furthermore, it implies their subdiffusive spreading.

DOI: 10.1103/PhysRevLett.110.060602 PACS numbers: 05.60.Gg, 71.10.Pm, 73.23.−b

The theory of quantum noise progressed rapidly during the last decades and it has become an important research area in the studies of transport in mesoscopic systems [1,2]. One of the key concepts of this field is the full counting statistics (FCS), giving the probability distribution of the charge transmitted through a conductor [3]. Non-Gaussian fluctuations of the FCS carry important information and the measurement of higher order cumulants has recently become accessible in a number of experiments on tunnel junctions [4,5], quantum dots [6,7], and quantum point contacts [8]. The FCS has also been proposed as a tool to extract the entanglement entropy [9] in terms of the measured cumulants [10–12].

Theoretically, the FCS is best understood for the transport of noninteracting electrons between conductance channels separated by a scatterer [3]. At zero temperature, an even simpler setup is to consider a one-dimensional system with perfect transmission, where the current is induced by preparing an initial state with two parts of the system having unequal particle densities. In this case, the complete time evolution of the FCS can be followed [13,14] and interesting results (e.g., particle number fluctuations logarithmically growing with time [14,15]) can be obtained.

The above setup with a steplike initial density is also remarkable because, due to the density bias, a front builds up and penetrates ballistically into the low density region [16]. This front displays an intriguing staircaselike fine-structure in the density [17] which has been also observed in the fronts of various quantum spin chains and in equivalent fermionic systems [18–21]. For free fermions, the fine structure appears to be related to the curvature of the single-particle dispersion around the Fermi points and thus cannot be accounted for in the usual semiclassical picture. Nevertheless, the staircase appearance of the front suggests a particle interpretation [17] and thus the FCS appears as a natural candidate for exploring the details of quantum fronts.

Our aim here is to probe the quantum noise in the front region by developing the FCS in a frame comoving with the edge of the front. For the free fermion case, our main result is the discovery of a connection between the FCS at the front edge and the distribution functions of the largest eigenvalues of the Gaussian unitary random matrix ensemble. This result allows us to characterize the front in terms of particles whose statistics, and in particular, their order statistics can be derived exactly.

The system under consideration is an infinite chain of free spinless fermions described by the Hamiltonian

$$\hat{H} = -\frac{1}{2}\sum_{m=-\infty}^{\infty}(c_m^\dagger c_{m+1} + c_{m+1}^\dagger c_m), \tag{1}$$

where $c_m^\dagger$ is a fermionic creation operator at site m. Initially, all the sites with $m \le 0$ are filled while those with $m > 0$ are empty and thus the correlations at time $t = 0$ are given by

$$\langle c_m^\dagger c_n\rangle = \begin{cases} \delta_{mn} & m, n \le 0 \\ 0 & \text{else} \end{cases}. \tag{2}$$

Since $\hat{H}$ is diagonalized by a Fourier transform with a single-particle spectrum $\omega_q = -\cos q$, the time evolution of the Fermi operators $c_m(t)$ can be obtained in terms of Bessel functions $J_m(t)$ as

$$c_m(t) = \sum_{j=-\infty}^{\infty} i^{j-m} J_{j-m}(t) c_j. \tag{3}$$

The step function in the density $n_m(t)$ spreads out ballistically and for $m > 0$ is given by [16]

$$n_m(t) = \langle c_m^\dagger(t) c_m(t)\rangle = \frac{1}{2}[1 - J_0^2(t)] - \sum_{k=1}^{m-1} J_k^2(t) \tag{4}$$

with snapshots of the density profile shown on Fig. 1. The curves for different times collapse in the bulk by choosing the scaling variable m/t, and the emerging profile can be understood by semiclassical arguments [15]. However, there is a nontrivial staircase structure emerging around the edge of the front, shown by the shaded areas in Fig. 1. The size of the edge region was found to scale with $t^{1/3}$ and it was argued that each step contains one particle [17]. Since the origin of this behavior cannot be captured by a semiclassical treatment, a more detailed understanding will be obtained by looking at the FCS which includes all the higher order correlations of the particle number.

The FCS is defined through the generating function

$$\chi(\lambda, t) = \langle \exp[i\lambda \hat{N}_A(t)] \rangle, \tag{5}$$

where $\hat{N}_A(t) = \sum_{m\in A} c_m^\dagger(t) c_m(t)$ is the particle number operator in subsystem A at time t. The subsystem will be chosen to include only the edge of the front and thus A itself is time dependent. The generating function can be written as a determinant [13,14]

$$\chi(\lambda, t) = \det[\mathbf{1} + (e^{i\lambda} - 1)\mathbf{C}(t)], \tag{6}$$

where $\mathbf{C}(t)$ is the reduced correlation matrix at time t with matrix elements $C_{mn}(t) = \langle c_m^\dagger(t) c_n(t) \rangle$ restricted to the subsystem, $m, n \in A$, while $\mathbf{1}$ is the identity matrix on the same interval. For the step initial condition one obtains the matrix elements as [16]

$$C_{mn}(t) = \frac{i^{n-m} t}{2(m-n)} [J_{m-1}(t) J_n(t) - J_m(t) J_{n-1}(t)]. \tag{7}$$

For convenience, we define $\tilde{C}_{mn}(t)$ by dropping the phase factor i^{n-m} in Eq. (7) which corresponds to a simple unitary transformation of the matrix $\mathbf{C}(t)$ and thus leaves $\chi(\lambda, t)$ invariant. Note that $\tilde{\mathbf{C}}(t)$ has exactly the same form as the ground-state correlation matrix of a free fermion chain with a gradient chemical potential [22]. Thus our results can be directly applied to the static interface problem as well.

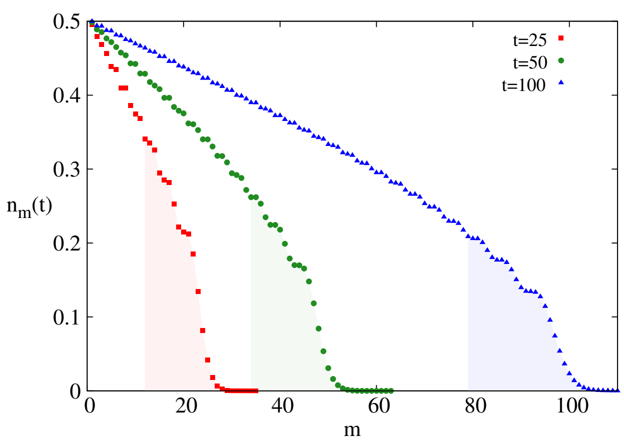

FIG. 1 (color online). Density profiles $n_m(t)$ at increasing times. The edge of the front with the emerging staircase structure is shown by the shaded region. The profile for $m \leq 0$ is given by $n_m(t) = 1 - n_{1-m}(t)$ and is not shown.

In order to explore the edge region of the front which scales as $t^{1/3}$, we introduce scaling variables x and y through $m = t + 2^{-1/3} t^{1/3} x$ and $n = t + 2^{-1/3} t^{1/3} y$. We also use the identity $J_{m-1}(t) = \dot{J}_m(t) + \frac{m}{t} J_m(t)$ to rewrite $\tilde{C}_{mn}(t)$ in terms of Bessel functions and their time derivatives as

$$\frac{t}{2(m-n)} \Big[\dot{J}_m(t) J_n(t) - J_m(t) \dot{J}_n(t) \Big] + \frac{1}{2} J_m(t) J_n(t). \tag{8}$$

In the asymptotic regime $t \to \infty$, one has the following forms [23] for the Bessel function and its time derivative

$$J_m(t) \approx 2^{1/3} t^{-1/3} \mathrm{Ai}(x), \quad \dot{J}_m(t) \approx -2^{2/3} t^{-2/3} \mathrm{Ai}'(x), \tag{9}$$

and the other pair of equations is obtained by interchanging $m \to n$ and $x \to y$. Substituting into Eq. (8) one arrives at

$$\tilde{C}_{mn}(t) \approx 2^{1/3} t^{-1/3} K(x, y) + 2^{-1/3} t^{-2/3} \mathrm{Ai}(x) \mathrm{Ai}(y), \tag{10}$$

where

$$K(x, y) = \frac{\mathrm{Ai}(x)\mathrm{Ai}'(y) - \mathrm{Ai}'(x)\mathrm{Ai}(y)}{x - y}. \tag{11}$$

The factor $2^{1/3} t^{-1/3}$ in the first term of Eq. (10) accounts for the change of variables while the other term vanishes in the scaling limit. Therefore, the reduced correlation matrix is turned into an integral operator and the generating function is given by the Fredholm determinant

$$\chi(\lambda, s) = \det[1 + (e^{i\lambda} - 1)K], \tag{12}$$

where s denotes the scaled left endpoint of the domain $A = (s, \infty)$ over which the kernel $K(x, y)$ is defined.

The Airy kernel, Eq. (11), is well known in the theory of random matrices from the Gaussian unitary ensemble (GUE). Namely, it appears in the level spacing distribution at the edge of the spectrum [24,25]. The bulk eigenvalue density of $N \times N$ GUE matrices is described by the so-called Wigner semicircle with the endpoints at $\pm\sqrt{2N}$. However, in order to capture the fine structure of the edge of the spectrum one has to magnify it by choosing the scaling variable $\sqrt{2N} + 2^{-1/2} N^{-1/6} s$. Then the probability that exactly n eigenvalues lie in the interval (s, ∞) is given by the expression [24,25]

$$E(n, s) = \frac{(-1)^n}{n!} \frac{d^n}{dz^n} \det(1 - zK) \bigg|_{z=1}. \tag{13}$$

We can easily prove now that the eigenvalue statistics, Eq. (13), at the edge of the GUE spectrum is identical to that of the quantum front with n being the number of particles. Indeed, the generating function of Eq. (13) is obtained by a Fourier transform and can be written as

$$\chi(\lambda, s) = \exp\left(-e^{i\lambda}\frac{d}{dz}\right)\det(1 - zK)\Big|_{z=1}. \quad (14)$$

Here, one can notice the operator of the translation which acts as $\exp(a\frac{d}{dz})f(z) = f(z + a)$ on any analytical function. Translating the argument and setting $z = 1$ afterwards, one immediately recovers the previous result, Eq. (12). We have thus mapped the FCS of the quantum front to the well studied problem of GUE edge eigenvalue statistics. One should point out, however, that while the edge region of the front widens with time, the edge of the random matrix spectrum shrinks with the matrix size and thus the correspondence is valid only after proper rescaling.

As an application of the mapping, we revisit the question of interpretation of the edge density profile in terms of single particles [17], and we also obtain the order statistics of the particles. In the random matrix language, the probability density of the nth largest eigenvalue for GUE random matrices is given by [24]

$$F(n, x) = \sum_{k=0}^{n-1}\frac{dE(k, x)}{dx}. \quad (15)$$

In addition, one has the following sum rules [25]:

$$\sum_{k=0}^{\infty}E(k, x) = 1, \qquad \sum_{k=0}^{\infty}kE(k, x) = \mathrm{Tr}K \quad (16)$$

with obvious probabilistic interpretations. Using the above sum rules, one arrives at the scaled density of eigenvalues as a sum of single eigenvalue densities

$$\sum_{n=1}^{\infty}F(n, x) = -\sum_{k=0}^{\infty}k\frac{dE(k, x)}{dx} = \rho(x), \quad (17)$$

where

$$\rho(x) = K(x, x) = [\mathrm{Ai}'(x)]^2 - x\mathrm{Ai}^2(x) \quad (18)$$

is obtained from Eq. (11) by taking the limit $x \to y$.

The results, Eqs. (15) and (17), have clear interpretations in the particle picture. Namely, the probability distribution of the nth eigenvalue $F(n, x)$ is the probability distribution of the scaled position of the nth particle. Thus the functions $F(n, x)$ provide us with the order statistics of the rightmost particles in the front with $F(1, x)$ being the Tracy-Widom distribution [24]. Furthermore, the sum of the probability distributions $F(n, x)$ gives us the scaled density $\rho(x)$ of particles in the front. Figure 2 shows the distributions of the first six particles obtained by a powerful numerical method for the evaluation of Fredholm determinants [26]. The sum of them, shown by the dashed line, deviates from $\rho(x)$ only at $x \approx -8$.

It is remarkable that the description of the front we found is consistent with a classical particle picture. One should also remember, however, that the position of the particles spreads out as $t^{1/3}$ in the original (unscaled) variables. This subdiffusive spreading has a quantum origin; namely, it follows from the cubic nonlinearity of the dispersion around the Fermi points.

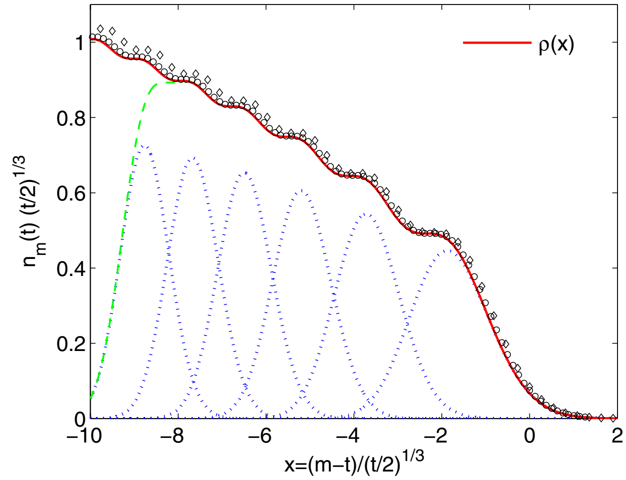

FIG. 2 (color online). Rescaled density near the edge of the front for $t = 100$ (diamonds) and $t = 1000$ (circles). The solid (red) line shows the scaling function $\rho(x)$ while the distribution functions of the nth particle for $n = 1, \ldots, 6$ are shown by the dotted (blue) lines. The dashed (green) line is the sum of the $F(n, x)$.

Additional information on the front region is contained in the cumulants κ_n of the FCS. They can be obtained from logarithmic derivatives $\kappa_n = (-i\partial_\lambda)^n \ln\chi(\lambda, s)|_{\lambda=0}$ of the generating function, Eq. (12). Using properties of Fredholm determinants, the cumulant generating function reads

$$\ln\chi(\lambda, s) = \sum_{k=1}^{\infty}(-1)^{k+1}\frac{\mathrm{Tr}K^k}{k}(e^{i\lambda} - 1)^k, \quad (19)$$

where the trace is defined as

$$\mathrm{Tr}K^k = \int_s^\infty dx_1 \ldots dx_k K(x_1, x_2)\ldots K(x_k, x_1). \quad (20)$$

The first two cumulants, corresponding to the total number and to the fluctuations of the particle number, have simple forms $\kappa_1 = \mathrm{Tr}K$ and $\kappa_2 = \mathrm{Tr}K(1 - K)$, respectively. In general, carrying out the traces in κ_n is difficult and would require knowledge of the eigenvalues of the kernel. Having the spectrum would also give access to more complicated quantities of interest such as the entanglement entropy [10–12]

$$S = -\mathrm{Tr}[K\ln K + (1 - K)\ln(1 - K)]. \quad (21)$$

Even though there exists a differential operator commuting with K [24], the solution of its eigenproblem is not known and the analytic calculation of κ_2 and S remains a challenge.

Numerically, we can calculate κ_2 and S from the matrix representation of the FCS given in Eq. (6), using matrices

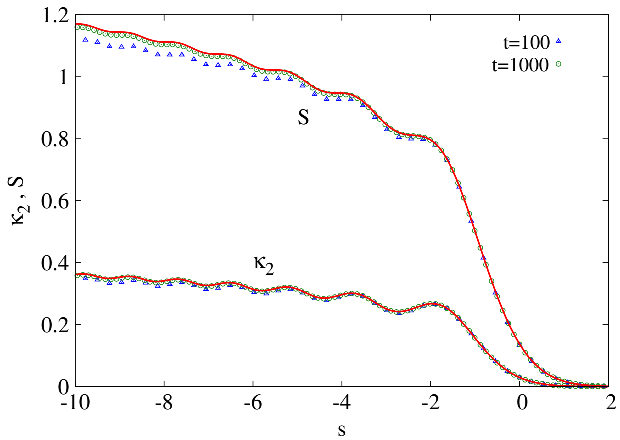

FIG. 3 (color online). Entanglement entropy S (upper symbols) and particle-number fluctuations κ_2 (lower symbols) in the edge region for different times as functions of the scaled coordinate s. The solid (red) lines are the $t \to \infty$ scaling functions.

of sufficiently large size. The results are shown in Fig. 3 for different times, plotted against the scaling variable s. One can see that the convergence to the $t \to \infty$ limit is fast. Indeed, for $t = 1000$, we have a nearly perfect collapse onto the scaling functions $\kappa_2 = \mathrm{Tr}K(1 - K)$ and S given by Eq. (21) and evaluated by using the methods described in Ref. [26]. This gives us a further check on the scaling function of the FCS, Eq. (12). One should also note that both κ_2 and S inherit signatures of the discrete particle picture developed above.

We have found a direct correspondence between counting statistics of free fermions at the edge of an evolving quantum front and that of random matrix eigenvalues in GUE edge spectra. A similar correspondence between the equilibrium FCS of fermions in a line segment and the statistics of bulk eigenvalues in the GUE spectrum can also be recognized. Indeed, in a proper continuum limit, the FCS can again be written as the Fredholm determinant, Eq. (12), with the Airy kernel $K(x, y)$ replaced by the sine kernel [27,28] which is associated with the bulk spectra of GUE matrices. For fermions on a finite chain, the connection to random matrices was already pointed out in Ref. [29] where the Toeplitz determinant arising in the study of entanglement entropy was related to the eigenvalue statistics of the circular unitary ensemble (CUE). Note, however, that the CUE and the GUE statistics become identical in the bulk scaling limit [25].

Interestingly, the equilibrium statistics also appears in the context of our nonequilibrium problem if one considers a finite segment in the middle of the chain ($m, n \ll t$) in the limit $t \to \infty$. Then the matrix elements $C_{mn}(t)$ become independent of t and unitarily equivalent to the equilibrium correlations [16], as can be seen from an asymptotic expansion of the Bessel functions in Eq. (7). As discussed in the previous paragraph, this implies bulk GUE statistics for the FCS.

It would be important to check the universality of the edge behavior of quantum fronts. The simplest generalization would be to start from an initial state, where the left (right)-hand side of the chain is not completely filled (empty) [17] or the initial density profile is a smooth function [21]. In such cases the staircase structure has been found to be essentially unchanged. Moreover, a very similar structure of the magnetization front was observed in the transverse Ising model starting from a domain wall initial state [30]. One might expect that the FCS remains unchanged in the above cases.

Another important question is the role of interactions. Does the edge structure survive if one remains in the integrable Luttinger liquid regime? How robust is it against integrability breaking terms? Recently, a numerical technique was proposed [31] which might be suitable to attack these questions.

Finally, we mention an intriguing connection to the asymmetric exclusion process [32–34]. There, starting from a step initial condition, the distribution of particle positions can also be calculated [35]. One observes a $t^{1/2}$ scaling for the width of the distributions at the edge of the front, while the $t^{1/3}$ scaling and the Tracy-Widom distribution emerge towards the bulk where the exclusion interaction between the particles becomes more important. Although there is no one-to-one correspondence to our result, nevertheless one may ask whether the quantum effects due to the curvature in the spectrum could be described in terms of some generalized semiclassical picture, e.g., by introducing effective interactions between particles of different velocities.

This work was supported by the ERC grant QUERG and by the Hungarian Academy of Sciences through OTKA Grants No. K 68109 and No. NK 100296. We are indebted to Folkmar Bornemann for his help in using his Matlab toolbox for the numerical evaluation of distributions in random matrix theory [26].

[1] Y. M. Blanter and M. Büttiker, Phys. Rep. **336**, 1 (2000).
[2] *Quantum Noise in Mesoscopic Physics*, edited by Yu. V. Nazarov, NATO Science Series II, Vol. 97 (Kluwer, Dordrecht, 2003).
[3] L. S. Levitov and G. B. Lesovik, JETP Lett. **58**, 230 (1993).
[4] B. Reulet, J. Senzier, and D. E. Prober, Phys. Rev. Lett. **91**, 196601 (2003).
[5] Yu. Bomze, G. Gershon, D. Shovkun, L. S. Levitov, and M. Reznikov, Phys. Rev. Lett. **95**, 176601 (2005).
[6] T. Fujisawa, T. Hayashi, R. Tomita, and Y. Hirayama, Science **312**, 1634 (2006).
[7] S. Gustavsson, R. Leturcq, B. Simovič, R. Schleser, T. Ihn, P. Studerus, K. Ensslin, D. C. Driscoll, and A. C. Gossard, Phys. Rev. Lett. **96**, 076605 (2006).
[8] G. Gershon, Yu. Bomze, E. V. Sukhorokov, and M. Reznikov, Phys. Rev. Lett. **101**, 016803 (2008).

[9] P. Calabrese, J. Cardy, and B. Doyon, J. Phys. A **42**, 500301 (2009).
[10] I. Klich and L. Levitov, Phys. Rev. Lett. **102**, 100502 (2009).
[11] H. F. Song, C. Flindt, S. Rachel, I. Klich, and K. Le Hur, Phys. Rev. B **83**, 161408(R) (2011).
[12] P. Calabrese, M. Mintchev, and E. Vicari, Europhys. Lett. **98**, 20003 (2012).
[13] I. Klich, in *Quantum Noise in Mesoscopic Physics*, edited by Yu. V. Nazarov, NATO Science Series II, Vol. 97 (Kluwer, Dordrecht, 2003), pp. 397–402.
[14] K. Schönhammer, Phys. Rev. B **75**, 205329 (2007).
[15] T. Antal, P. L. Krapivsky, and A. Rákos, Phys. Rev. E **78**, 061115 (2008).
[16] T. Antal, Z. Rácz, A. Rákos, and G. M. Schütz, Phys. Rev. E **59**, 4912 (1999).
[17] V. Hunyadi, Z. Rácz, and L. Sasvári, Phys. Rev. E **69**, 066103 (2004).
[18] D. Gobert, C. Kollath, U. Schollwöck, and G. Schütz, Phys. Rev. E **71**, 036102 (2005).
[19] T. Platini and D. Karevski, J. Phys. A **40**, 1711 (2007).
[20] J. Lancaster and A. Mitra, Phys. Rev. E **81**, 061134 (2010).
[21] E. Bettelheim and L. Glazman, arXiv:1209.1881.
[22] V. Eisler, F. Iglói, and I. Peschel, J. Stat. Mech. (2009) P02011.
[23] *Handbook of Mathematical Functions*, edited by M. Abramowitz and I. A. Stegun (Dover, New York, 1964).
[24] C. A. Tracy and H. Widom, Commun. Math. Phys. **159**, 151 (1994).
[25] M. L. Mehta, *Random Matrices* (Elsevier, Amsterdam, 2004), 3rd ed.
[26] F. Bornemann, Markov Proc. Relat. Fields **16**, 803 (2010).
[27] A. G. Abanov, D. A. Ivanov, and Y. Qian, J. Phys. A **44**, 485001 (2011).
[28] D. A. Ivanov, A. G. Abanov, and V. V. Cheianov, arXiv:1112.2530.
[29] J. P. Keating and F. Mezzadri, Phys. Rev. Lett. **94**, 050501 (2005).
[30] T. Platini and D. Karevski, Eur. Phys. J. B **48**, 225 (2005).
[31] V. Zauner, M. Ganahl, H. G. Evertz, and T. Nishino, arXiv:1207.0862.
[32] K. Johansson, Commun. Math. Phys. **209**, 437 (2000).
[33] M. Prähofer and H. Spohn, Physica (Amsterdam) **279A**, 342 (2000).
[34] T. Sasamoto, J. Stat. Mech. (2007) P07007.
[35] C. A. Tracy and H. Widom, Commun. Math. Phys. **290**, 129 (2009).